Atom-Based Modeling of Amorphous 1,4-*cis*-Polybutadiene

Yong Li and Wayne L. Mattice*

Institute of Polymer Science, University of Akron, Akron, Ohio 44325-3909

Received April 6, 1992

ABSTRACT: The structure of amorphous 1,4-*cis*-polybutadiene is simulated with molecular mechanics and molecular dynamics subjected to periodic boundary conditions. All hydrogen atoms are explicitly taken into account. By means of the relaxation strategy which has been developed in this work, the low-energy states of relatively large systems can be reached within an acceptable computational time. With the five simulated structures, the distribution of bond angles, distribution of dihedral angles, and correlated distribution of pairs of neighbor dihedral angles, as well as cohesive energy, solubility parameter, and atom pair radial distribution functions, are evaluated and discussed.

Introduction

Because of their widespread areas of application, amorphous polymers have played an important role in polymer science. The structures of amorphous polymers, which fundamentally fix the properties, have been intensively investigated experimentally as well as theoretically in the past.[1-3] In spite of the efforts made in this field many problems still remain. For example, one is interested in (1) the order in the amorphous state, if it exists, (2) the distribution of free volume, (3) the conformation of polymer chains in the bulk, etc. Molecular modeling provides the opportunity for studying the structures of amorphous polymers at the level of individual atoms. Detailed information about the arrangement of molecules and chain segments in the amorphous state can be obtained.[4]

An important advance in computer simulation of amorphous polymer materials was carried out by Theodorou and Suter.[5-7] They evaluated the static and mechanical properties of glassy atactic polypropylene by using a clever strategy for molecular mechanical energy minimization.[5] After this, Suter and co-workers used the above method to study the structures of poly(vinyl chloride)[8] and polycarbonate.[9-11] In their simulation, no bond stretching or bond bending was considered and the density was fixed. Rigby and Roe used molecular dynamics to simulate the structure of the melt and glass of short-chain molecules.[12-15] During the stepwise cooling in their simulation, the volume of their structures as a function of temperature showed a crossover, which was interpreted as the glass transition temperature. Above this temperature the structure is thought of as a melt, and below this temperature it is thought of as a glass. Using stochastic dynamics and the Monte Carlo method, Winkler et al.[16] simulated the structure of *n*-alkane melts and compared the simulation results with the rotational isomeric states model calculation. The last two groups incorporated the bond stretching and bond bending into their energy calculations, but the methylene groups were considered as spherical balls. Recently, simulation of amorphous aromatic polysulfone was performed by Fan and Hsu.[17] In their study of systems with a relatively low degree of polymerization (i.e., 10), all effects of bond stretching and bond bending were considered.

We report here the first results of our molecular modeling of amorphous polybutadienes. This polymer is selected for study because of its obvious importance to the tire and rubber industry and because we have available a force field that is appropriate for use with this polymer, as shown by recent works in our group.[18-20] The local structure and the packing of a system with bulk density strongly depend on the detailed structure of the molecules. Hence, we take all hydrogen atoms into account to avoid any error which may arise from neglecting the nonspherical geometry of methylene and methine groups. This more precise approach to the real structure is at expense of more computational time, which is needed for the generation of the structures.

Structure Model

The molecular mechanics and molecular dynamics in this study were performed using Version 2.20 of Polygraf provided by Polygen/Molecular Simulations Inc. The potential energy of the system, E, was calculated as

$$E = E_{\text{stretching}} + E_{\text{bending}} + E_{\text{torsion}} + E_{\text{inversion}} + E_{\text{vdW}} \quad (1)$$

Parameters for bond bending and torsion in the Dreiding force field were modified particularly for use to polybutadiene, as described in a previous work.[18]

A polymer chain with a degree of polymerization of 99 was generated with all CH=CH double bonds in the cis conformation, corresponding to pure *cis*-polybutadiene (Figure 1). As mentioned above, all hydrogen atoms were explicitly taken into consideration. The polymer chain has 395 backbone bonds and 992 atoms.

The amorphous bulk structure of polybutadiene was simulated with cubic periodic boundary conditions, which has been successfully used to simulate glassy bulk polymers and polymer melts by several research groups.[5,12,16,17] By setting the density of the bulk polybutadiene at 0.89 g/cm^3,[21] the cubic amorphous cell has an edge length of 21.54 Å. The amorphous structure in the cell was generated by using the Monte Carlo method for dihedral angles of all rotatable backbone bonds at 300 K. The polymer chain "grows" in the cubic cell bond by bond. If the chain passes through one face of the cell, it would reenter the cell through the opposite face. To enhance the efficiency, the van der Waals radii of all atoms were reduced to 30% of their actual values during the whole growing process. The size and the shape of the cubic cell were kept unchanged during the growing process as well as during the later energy minimization and molecular dynamics runs. If the density which was set before the growing process has a reasonable value, the rigid cell saves a lot of computational time.

Using the method described above, five amorphous structures with different conformations were generated.

The initial structures have very high potential energy because of the crude growing process and the resulting inhomogeneity in the cell.[5] The relaxation of these high-energy structures should be handled with care. Because

0024-9297/92/2225-4942$03.00/0

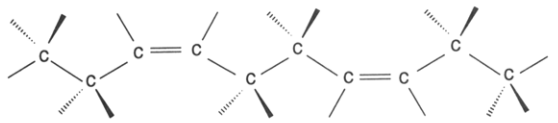

Figure 1. Structure of *cis*-polybutadiene.

Table I
Energies of Relaxed Structures [kcal/mol (structure)]

	structure no.					
	1	2	3	4	5	std dev
total	551.10	575.58	571.04	558.63	573.97	±10.09
stretching	87.84	88.23	90.33	89.26	86.58	±1.48
bending	250.27	248.34	252.32	253.64	245.50	±3.43
torsion	162.03	181.11	172.19	162.76	172.30	±7.12
inversion	2.60	3.11	3.17	2.70	3.25	±0.29
vdW	48.34	54.78	53.03	50.27	66.33	±7.92

of its many degrees of freedom, the energy hypersurface of such a system is rough and has a great number of local minima. A simple straightforward molecular mechanics energy minimization will lead the system to the nearest local minimum, which still has an unreasonably high potential energy. The system will be trapped in this high-energy local minimum. Therefore in the literature great efforts were made to get a relative low-energy conformation of the system.[5,8,10]

In this study we used a three-step strategy to let the systems relax: step 1, the potential energy of the initial structure is minimized using the conjugate gradient method; step 2, the energy-minimized structure is heated step by step from 0 K to a very high temperature (in this case 500–1000 K) and a molecular dynamics run is performed at the high temperature; step 3, the conformation with the lowest total potential energy during the molecular dynamics duration is selected, and the potential energy of this structure is minimized again as in step 1.

The criterion of convergence for the conjugate gradient method used in steps 1 and 3 is a root mean square force less than 0.1 kcal mol^{-1} Å^{-1}. A standard Verlet algorithm with a time step of 10^{-15} s was used in step 2. The temperature step used for heating is 50–100 K, and the length of a molecular dynamics run is 5–10 ps.

We used all five generated structures with low and high initial potential energy for the relaxation process and all five structures after relaxation for the analysis. We believe that a good relaxation strategy should be able to bring all possible initial structures generated as described above to a reasonable low-energy state.

It must be noted that the unusually high temperature used in the molecular dynamics in step 2 is on the one hand necessary, to give the system enough energy to surmount the energy barriers between local minima, and on the other hand desirable, to reduce the computational time. This high temperature should not be interpreted and compared with a polymer system at such a high temperature in reality. It is only a computational technique. We can do it with our computer-simulated systems because we keep the volume of our systems constant. It is this artificial high density and the absence of a bond dissociation term in the force field which keep our system stable at such an unrealistically high temperature. This is also one reason for us to choose molecular mechanics and molecular dynamics at constant volume instead of at constant pressure for the relaxation process in our present study.

The total potential energies and their compositions for the five relaxed structures are listed in Table I. The very small differences of total energy (~4%) among the five structures and the relatively small internal stresses which

Table II
Internal Stresses of Relaxed Structures (GPa)

	structure no.				
	1	2	3	4	5
σ_{xx}	0.056	−0.076	−0.109	−0.023	−0.049
σ_{xy}	0.042	−0.017	−0.010	0.023	0.016
σ_{xz}	−0.040	−0.059	0.017	−0.015	0.077
σ_{yy}	−0.104	−0.068	0.018	0.012	−0.126
σ_{yz}	−0.074	−0.034	−0.024	0.003	−0.038
σ_{zz}	−0.016	−0.034	0.055	−0.028	−0.242

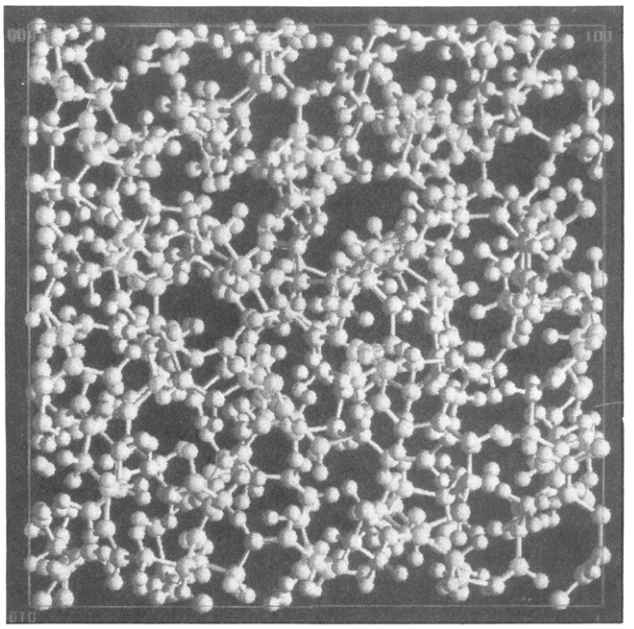

Figure 2. Amorphous cell of one relaxed structure (no. 2). The atoms are shown as spheres with radii smaller than the van der Waals radii to permit viewing of all atoms in the cell.

are listed in Table II indicate that these structures are well relaxed. The components of the internal stress tensor are sums of forces acting on each atom, calculated as[17]

$$\sigma_{ij} = \sum_{kl} (r_i^k - r_i^l) f_j^{kl} / 2V \qquad (2)$$

where r_i is the coordinate of the kth or lth atom in the i direction, f_j is the jth component of the force acting between the two atoms, and V is the volume of the structure. The standard deviations in the last column in Table I show that the torsional and the van der Waals (vdW) energies are responsible for most of the variation in the total energy.

The small internal stresses show that the value of the density, which was set before the generation and kept constant during the whole relaxation process, is reasonable. Figure 2 shows one of the five amorphous cells after relaxation. Unlike the initial structures generated with the random method,[5] the distribution of the atoms in our relaxed cell is very homogeneous.

For a comparison between chains in bulk structures and single chains, we generated also five single chains in different conformations without the periodic cell and then minimized the energy of the chains.

Results and Discussion

Chain Conformational Properties. The chain conformational characteristics can be divided into two categories: (1) whole-chain properties and (2) bond or bond pair properties. The first category includes quantities like the radius of gyration, the mean square end-to-end distance, etc., which depend on the entire polymer

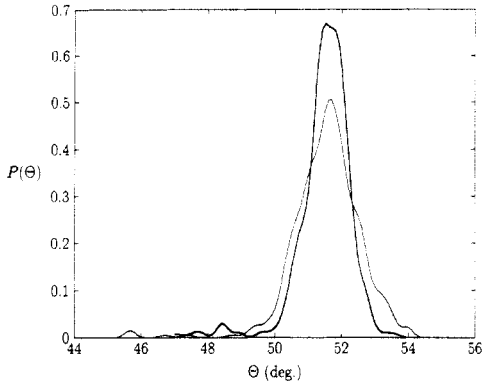

Figure 3. Distribution of the supplement of the bond angle CH=CH–CH_2 for bulk (thin line) and single chain (thick line).

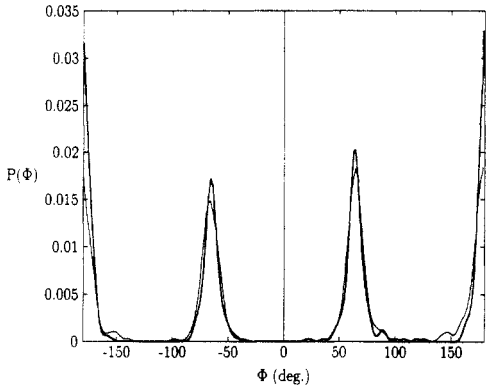

Figure 4. Distribution of the dihedral angle at bond CH_2–CH_2 for bulk (thin line) and single chain (thick line).

chain. Because of the small number of model structures which are generated in this study, it would be hard to place confidence in any analysis of such properties. In fact, these whole-chain properties are controlled by the statistical distribution of quantities of each bond or bond pair in the chain. Only these bond and bond pair properties will be discussed in the following. The comparison between packed structures and single chains minimized in a vacuum permits an assessment of whether intermolecular interactions in the system at bulk density modify the local conformation.

The distributions of the supplement of the bond angles CH=CH–CH_2 in the bulk structures and single chains are shown in Figure 3. The calculations of the distributions take all 990 bond angles CH=CH–CH_2 in the five different structures in the corresponding case into account. Because of the relatively large force constant used in the simulation, also, in reality, the distributions of the bond angles are very narrow around its mean value about 51.6°. The standard deviation for this distribution is 1.02°. In the case of the single chain there is no intermolecular interaction in the system, and therefore the distribution of the bond angles is only controlled by the intramolecular interaction. Because of the strong intermolecular interactions due to the high compactness in the bulk state, the distribution of the bond angles is broader than for the single chain.

The distributions of the dihedral angles of the bonds CH_2–CH_2 in the bulk and in the single chains are shown in Figure 4. Both distributions show three broad peaks located at trans (180°), gauche$^+$ (+60°), and gauche$^-$ (−60°). Because of the limited number of methylene–methylene bonds (i.e., 490), the identity in peak size for gauche$^+$ and gauche$^-$ demanded by the symmetry of the rotation potentials is not precisely achieved. In their

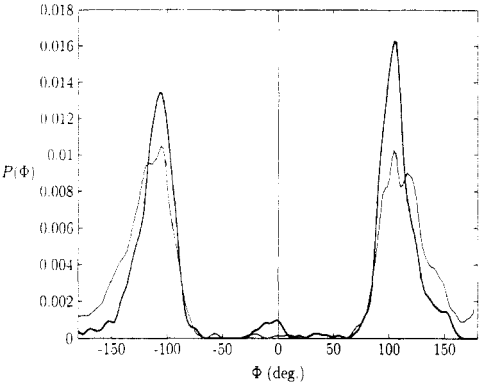

Figure 5. Distribution of the dihedral angle at bond CH–CH_2 for bulk (thin line) and single chain (thick line).

Table III
Populations of CH_2–CH_2 Dihedrals

	trans[a]	gauche$^+$ [b]	gauche$^-$ [c]
bulk	0.400	0.324	0.276
single chain	0.434	0.306	0.260
theor model[d]			
E_σ = 100 cal/mol	0.368	0.316	0.316
E_σ = 0 cal/mol	0.333	0.333	0.333

[a] Defined as the range of 120 to 180° and −180 to −120°. [b] Defined as the range of 0 to 120°. [c] Defined as the range of −120 to 0°. [d] Abe, Y.; Flory, P. J. *Macromolecules* **1971**, *4*, 219.

rotational isomeric states calculations, Mark[22] and Abe and Flory[23] took these three locations as rotational isomeric states for the dihedral angle between two methylene groups. The population probabilities of these three rotational isomeric states calculated from them for the ideal chain and those from our simulations of the bulk state and single chain are listed in Table III.

The assignment of rotational isomeric states for the methine–methylene bonds is very interesting. Earlier works[24,25] showed that these dihedral angles may have cis (0°), skew$^+$ (+120°), and skew$^-$ (−120°) as rotational isomeric states. In our simulation we also used a threefold potential with minima which are located on these three positions. In spite of this threefold potential, both distributions show only two significant population areas around +105° (skew$^+$) and −105° (skew$^-$) (Figure 5). For single chains the distribution also has a very small peak around 0° (cis). The disappearance of the cis conformation of the methine–methylene bonds is caused by steric repulsions of groups which are separated by the cis double bond and its two nearest methine–methylene bonds.[23]

Because of the relatively small energy barriers[26] between the different conformations of the methine–methylene bonds, a much larger difference between the distribution of the bulk state and the single chain can be found. The curve for the bulk state in Figure 5 is not only broader, as other distributions for the bulk state, but also changes its shape. The single peak at skew$^+$ as well as skew$^-$ for the single chain splits into two peaks in the case of the bulk state. While the higher of the two peaks has the same location as the peak for the single chain, the second peak shifts to a position (about ±120°) which is nearer to the trans conformation. We do not think that this splitting is an effect of bad statistics because it happens symmetrically in both the skew$^+$ and skew$^-$ conformations. Because we did not use the rotational isomeric states for generating our initial structures, we had a nearly random distribution of the dihedrals of the methine–methylene bonds in the initial structures. Hence, it cannot be the case that some of the bonds have been trapped in their unfavorable beginning conformations because of a bad

Table IV
Populations of CH_2–CH Dihedrals

	cis[a]	skew+ [b]	skew− [c]	trans[d]
bulk	0.007	0.452	0.444	0.097
single chain	0.028	0.491	0.453	0.028
theor model[e]	0	0.476	0.476	0.048

[a] Defined as the range of −60 to +60°. [b] Defined as the range of 60 to 150°. [c] Defined as the range of −150 to −60°. [d] Defined as the range of −180 to −150° and 150 to 180°. [e] Abe, Y.; Flory, P. J. *Macromolecules* **1971**, *4*, 219.

relaxation strategy and therefore give rise to the second peak in the distribution. As a logical conclusion, this conformational difference between the bulk and the single chain must be of intermolecular origin. The intermolecular interactions do not shift the conformation directly. They screen the intramolecular nonbonded interactions which shift the methine–methylene bond conformation to the minima of the intramolecular potential energy (about ±105°, as seen for the single chains). Therefore in the bulk state, for some of the methine–methylene bonds, their dihedrals are shifted to the conformation with the lowest intramolecular potential energy like in the single chains and cause the higher peak in the distribution. For some of the bonds, the intramolecular nonbonded interactions are screened by the intermolecular interactions, and their dihedrals take the conformations ±120°, which have the lowest $E_{torsion}$ in eq 1, instead of the minima of whole intramolecular interactions and cause the lower peak of the distribution.

As suggested by Mark,[22] our simulation results (Table IV)also show that a significant contribution to the conformation distribution occurs in the vicinity of trans (0°), especially in the case of the bulk state. For this reason, Abe and Flory[23] took the trans conformation instead of the cis conformation, in addition to the two skew conformations, as a rotational isomeric state in their calculations.

The other interesting statistical quantities of chain conformation are the correlated distributions of dihedral angle pairs. Generally, the rotation of a bond in a polymer chain is also related to the conformations of the bonds in its neighborhood because of the steric repulsion of groups separated by the bonds.[27] In a *cis*-polybutadiene chain groups of three rotatable bonds—methine–methylene, methylene–methylene, and methylene–methine—are separated by the double bonds with fixed conformation. We studied the bond conformation correlation among the bonds in the triplet bond group and the correlation between two neighbor groups, which is revealed as the distribution correlation between the methylene–methine bond and the methine–methylene bond, which are separated by a cis double bond. The population probability as a function of rotational angles of the methylene–methylene bond and the neighbor methylene–methine bond is shown in Figure 6. The barrier height for rotation about the methylene–methylene bond is much larger than for the methylene–methine bond; hence, in the direction parallel to the methylene–methylene axis, the peaks are narrower than in the perpendicular direction. All peaks in Figure 6 have a small shoulder, which has been seen in the distribution of rotational angles of the methylene–methine bond. Within the statistical error owing to the limited number of bond pairs, there is no conformational combination which is dominant for this bond pair in our structures. This result is in good agreement with the interaction energy calculation by Abe and Flory,[23] which predicts independence of the rotations about the single bonds for *cis*-polybutadiene.

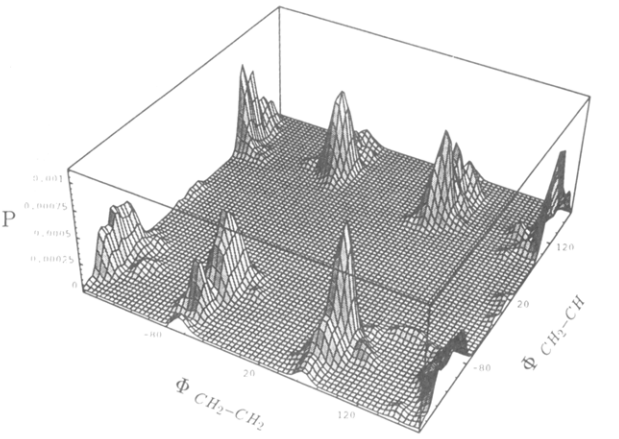

Figure 6. Correlated distribution of the dihedral angle of bonds CH–CH_2 and CH_2–CH_2 for bulk.

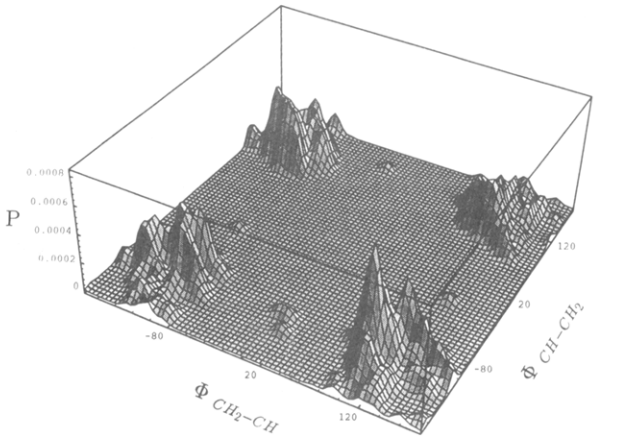

Figure 7. Correlation distribution of the dihedral angle of bonds CH_2–CH and CH–CH_2 for bulk.

The correlated distribution of the two methylene–methine bonds in different triplets is shown in Figure 7. Because of the nonrotatable double bond, which separates the two methylene–methine bonds, correlation of the conformations of these two bonds is expected. As shown in Figure 7, the populations in the four different quadrants have almost the same form. There is no evidence for any dominant conformation. This simulation result supports the conclusion of earlier theoretical investigations[22,23] that the proposed correlation between different triplets which are separated by a double bonds does not exist.

Cohesive Energy and Solubility Parameter. The most important advantage of the simulations of bulk density systems is the evaluating of the bulk properties like cohesive energy and radial distribution functions. A comparison of the calculated cohesive energy with the well-known experimental value is one criterion for evaluating how well our computer-simulated structures approximate the real amorphous polybutadiene structure.

The cohesive energy is defined as the work which is necessary if one takes a molecule away from the bulk. In our simulation, the cohesive energy is calculated as the energy difference between the amorphous structure and the parent chain. For our five relaxed structures we obtain an average energy

$$E_{bulk} = 5720 \pm 110 \text{ cal/mol (of repeat unit)} \quad (3)$$

and an average energy for the parent chains (calculated without the periodic boundary conditions)

$$E_{parent} = 9820 \pm 240 \text{ cal/mol} \quad (4)$$

The cohesive energy for our simulated amorphous struc-

tures is

$$E_{\text{cohesive}} = E_{\text{parent}} - E_{\text{bulk}} = 4100 \pm 350 \text{ cal/mol} \quad (5)$$

This result, which is evaluated from our simulation without any fit parameter, is in good agreement with the experimental value of 3980–4490 cal/mol.[21] From the cohesive energy we can also calculate the Hildebrand solubility parameter as

$$\delta = (E_{\text{cohesive}}/V_{\text{mol}})^{1/2} = 8.23 \pm 0.70 \text{ cal}^{1/2}/\text{cm}^{3/2} \quad (6)$$

which is well within the reported experimental values of 8.1–8.6 $\text{cal}^{1/2}/\text{cm}^{3/2}$.[21]

Radial Distribution Functions. The distribution of atoms in disordered matter, which includes amorphous polymers, can be specified by the atomic pair radial distribution functions.[28] These functions give the probabilities of finding a pair of atoms a distance r apart relative to the probabilities expected for a completely random distribution at the same density. The radial distribution functions can be evaluated with the simulated structures.[29] For our structures of polybutadienes there are three distinct atom pairs: the carbon–carbon, the carbon–hydrogen, and the hydrogen–hydrogen, if no distinctions between atoms of methylene groups and atoms of methine groups are made. A total radial distribution function (rdf) includes the contributions from all considered atom pairs in the structures. It is the distribution function which can be determined by experimental measurements, for example, by electron diffraction and X-ray diffraction experiment.[30,31] The total rdf can be divided into two contributions: one from the interference of atoms in the same chain, and the other from atoms in different chains. The intramolecular radial distribution function can also be measured experimentally, for example, by the neutron scattering method.[32,33] For our simulated structure the intramolecular radial distribution functions are calculated by taking the contributions from atom pairs which are in the same cell. The one not directly measurable by experiment is the intermolecular radial distribution function. However, these functions are most important because they describe the molecular arrangement in the bulk structure. Using molecular modeling we can evaluate these intermolecular rdf by considering the contribution from atom pairs of chain segments being in different cells. These atom pairs, which are placed in the same cell only by translation using periodic boundary conditions, are considered to be "intermolecular".

The calculated total radial distribution functions for the three different pairs of atoms in Figure 8 show similar behaviors. All of the three total distribution functions consist of two parts. The part from $r = 0$ Å to $r < 7$ Å varies strongly and has some very sharp peaks. The other part with $r > 7$ Å is nearly constant. A comparison with the intramolecular distribution functions (not depicted here) shows that the strongly varying parts of the total distribution functions arise from the intramolecular contributions. The sharp peaks correspond to the distances of atoms which are separated by one or two bonds. These distances do not depend on the chain conformation and give rise to the sharp peaks in the radial distribution functions. The part for long distance in the total distribution functions does not vary with the distance and has a value of unity, corresponding to a totally random distribution in this range. This indicates that in our simulated structures there is no correlation of distribution of atoms which are separated by a distance longer than 7 Å. No evidence of any "local order" (>7 Å) in our simulated amorphous structures can be found.

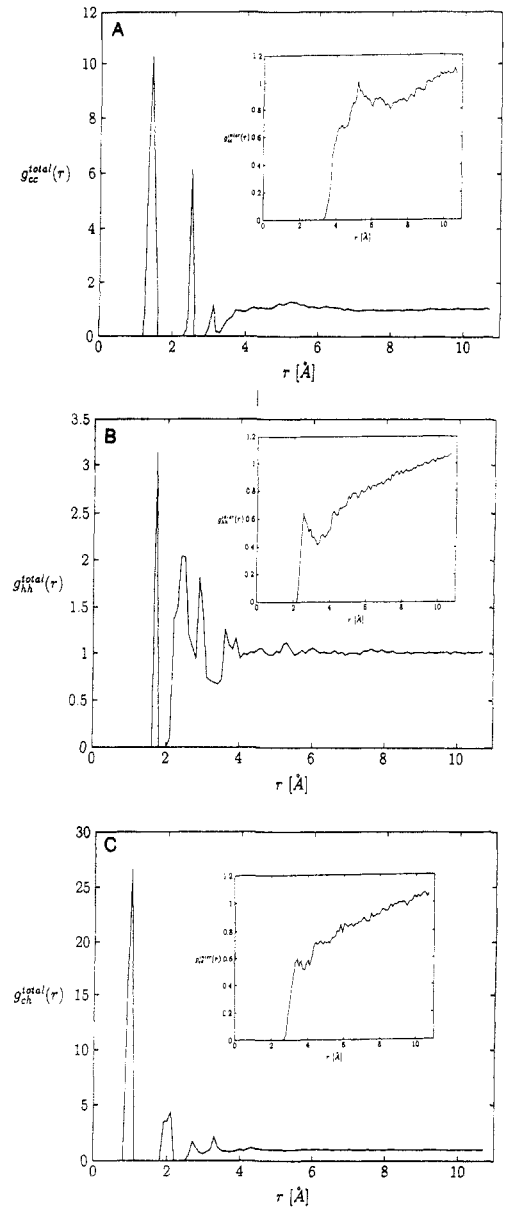

Figure 8. Total atom pair radial distribution function for (A) carbon–carbon, (B) hydrogen–hydrogen, and (C) carbon–hydrogen. The inserts depict the corresponding intermolecular atom pair radial distribution functions.

The intermolecular radial distribution functions for the three pairs of atoms are shown as inserts in Figure 8. In the long-distance range, all three distribution functions increase slowly, in compensation of the decreasing of the intramolecular distribution function in this range to keep the total distribution functions constant. The intermolecular radial distribution function for carbon–carbon atom pairs shows a more crowded range between 5 and 6 Å. This, like similar results from other groups,[5,10] could be an indication of enhanced order in this range. Because all carbon atoms in our case are in the backbone, this possible short-range order is also the order of arrangement of chain segments in our simulated amorphous structure. The intermolecular radial distribution function for the hydrogen–hydrogen pairs has its peak at about 2.5 Å, which is in the range of repulsive van der Waals interaction between two hydrogen atoms. The hydrogen atom is softer than the carbon atom; thus the filling of the volume with polymer chains in the bulk state is at the expense of hydrogen–hydrogen interaction.

Conclusions

Well-relaxed cubes, 21.54 Å on a side and with a bulk density of 0.89 g cm^{-3}, have been generated for amorphous (1,4-*cis*-polybutadiene). The Hildebrand solubility parameter deduced from these cubes is 8.23 ± 0.70 $cal^{1/2}$ $cm^{-3/2}$, which is in excellent agreement with the previously reported experimental values of 8.1–8.6 $cal^{1/2}$ $cm^{-3/2}$. Therefore the relaxed cubes have the correct cohesive energy. The distribution of rotational isomers at the rotatable bonds is in agreement with expectation. Radial distribution functions find no evidence for local order on a scale greater than about 7 Å. We conclude that the methodology employed for the generation of accurate atom-based molecular models of the amorphous polymer of butadiene is sound and that these models are appropriate initial structures for the computation of molecular dynamics trajectories, with the objective of characterizing local motions as a function of temperature.

Supplementary Material Available: Table of parameters used in the force field (1 page). Ordering information is given on any current masthead page.

Acknowledgment. This work was supported by Bridgestone/Firestone through EPIC.

References and Notes

(1) Walton, A. G., Ed. *Structure and Properties of Amorphous Polymers*; Elsevier: New York, 1980.
(2) Pethrick, R. A.; Richards, R. W., Eds. *Static and Dynamic Properties of the Polymeric Solid State*; D. Reidel: Dordrecht, Holland, 1982.
(3) Keinath, S. E.; Miller, R. L.; Ricke, J. K., Eds. *Order in the Amorphous "State" of Polymers*; Plenum Press: New York, 1987.
(4) Roe, R. J., Ed. *Computer Simulation of Polymers*; Prentice-Hall: Englewood Cliffs, NJ, 1991.
(5) Theordorou, D. N.; Suter, U. W. *Macromolecules* **1985**, *18*, 1467.
(6) Theordorou, D. N.; Suter, U. W. *Macromolecules* **1986**, *19*, 139.
(7) Theordorou, D. N.; Suter, U. W. *Macromolecules* **1986**, *19*, 379.
(8) Ludovice, P. J.; Suter, U. W. *Computer Simulation of Polymers*; Bicerano, J., Ed.; Marcel Dekker: New York, in press.
(9) Hutnik, M.; Argon, A. S.; Suter, U. W. *Macromolecules* **1991**, *24*, 5956.
(10) Hutnik, M.; Gentile, F. T.; Ludovice, P. J.; Suter, U. W.; Argon, A. S. *Macromolecules* **1991**, *24*, 5962.
(11) Hutnik, M.; Argon, A. S.; Suter, U. W. *Macromolecules* **1991**, *24*, 5970.
(12) Rigby, D.; Roe, R. J. *J. Chem. Phys.* **1987**, *87*, 7285.
(13) Rigby, D.; Roe, R. J. *J. Chem. Phys.* **1988**, *89*, 5280.
(14) Rigby, D.; Roe, R. J. *Macromolecules* **1989**, *22*, 2259.
(15) Rigby, D.; Roe, R. J. *Macromolecules* **1990**, *23*, 5312.
(16) Winkler, R. G.; Ludovice, P. J.; Yoon, D. Y.; Morawetz, H. *J. Chem. Phys.* **1991**, *95*, 4709.
(17) Fang, C. F.; Hsu, S. L. *Macromolecules* **1991**, *24*, 6244.
(18) Dodge, R.; Mattice, W. L. *Macromolecules* **1991**, *24*, 2709.
(19) Zhan, Y.; Mattice, W. L. *Macromolecules* **1992**, *25*, 1554.
(20) Zhan, Y.; Mattice, W. L. *J. Chem. Phys.* **1992**, *96*, 3279.
(21) Van Krevelen, D. W.; Hoftyzer, P. J. *Properties of Polymers—Their Estimation and Correlation with Chemical Structures*; Elsevier: New York, 1976.
(22) Mark, J. E. *J. Am. Chem. Soc.* **1966**, *88*, 4354.
(23) Abe, Y.; Flory, P. J. *Macromolecules* **1971**, *4*, 219.
(24) Allegra, G.; Flisi, U.; Crespi, G. *Macromol. Chem.* **1964**, *75*, 189.
(25) Allegra, G. *Makromol. Chem.* **1967**, *110*, 58.
(26) Hershbach, D. R. *Bibliography for Hindered Internal Rotation and Microwave Spectroscopy*; Lawrence Radiation Laboratory, University of California: Berkeley, CA, 1962.
(27) Flory, P. J. *Statistical Mechanics of Chain Molecules*; Interscience: New York, 1969.
(28) Hansen, J. P.; McDonald, I. R. *Theory of Simple Liquids*; Academic Press: London, 1986.
(29) Allen, M. P.; Tildesley, D. J. *Computer Simulation of Liquids*; Oxford University Press: Oxford, U.K., 1987.
(30) Wendorff, J. H. *Polymer* **1982**, *23*, 543.
(31) Lovell, R.; Mitchell, G. R.; Windle, A. H. *Faraday Discuss. Chem. Soc.* **1979**, *86*, 46.
(32) Kirste, R. G.; Kruse, W. A.; Ibel, K. *Polymer* **1975**, *16*, 120.
(33) Picot, C. In ref 1, p 127.

Registry No. 1,4-Butadiene (homopolymer), 9003-17-2.